Inclusive quasielastic electron scattering on ⁶He: a probe of the halo structure

E. Garrido and E. Moya de Guerra

Instituto de Estructura de la Materia, CSIC, Serrano 123, E-28006 Madrid, Spain

Abstract

We investigate inclusive electron scattering reactions on two-neutron halo nuclei in the quasielastic region. Expressions for the cross section and structure functions are given assuming that the halo nucleus can be described as a three-body system (core +n+n). The method is applied to ⁶He. We compute cross sections and structure functions, and investigate the kinematic conditions for which the observables are determined either by α -knockout or by halo neutron-knockout. The optimal kinematical domain to disantangle the momentum distributions of the various components of the three–body system ($q \lesssim 200 \text{ MeV/c}$ and $\omega < q^2/2M_N + 20 \text{ MeV}$) are explored.

PACS: 25.30.Fj, 25.10.+s, 21.45.+v

1 Introduction

Halo nuclei are the most intriguing objects among recent nuclear physics discoveries. Their small binding energies and large spatial extensions had no precedent and were totally unexpected in the realm of systems governed by the nuclear force. Borromean two–neutron halo systems show the additional peculiarity that the three–body (core+n+n) system completely falls apart when either of the three constituents drops out. Among the latter ⁶He ($\alpha+n+n$) is the one that is most stable and has been extensively studied. Since the initial discovery by Tanihata and collaborators [1,2], much progress has been made in theoretical [3–6] and experimental studies of halo nuclei. The available experimental information comes basically from nucleus–nucleus collisions [7–13]. This experimental information has the inherent difficulty of disentangling nuclear reaction mechanisms from nuclear structure effects. This is why the idea

of using nonhadronic probes to obtain complementary information on halo nuclei has been put forward.

The aim of this paper is to point out that, as for the case of stable nuclei, detailed information on charge density and momentum distributions in these systems can be obtained with electron beams. To this end we show theoretical results on differential cross sections and structure functions for the case of electron scattering from ⁶He. We do not discuss here important technical difficulties stemming from the short lives of halo nuclei and small production rates, which work against the feasibility of experiments involving measurements of cross sections for electron scattering from a halo–nucleus secondary beam. We just mention that in spite of these difficulties such experiments are in project at RIKEN [14], and are also being considered at GSI and Mainz.

To our knowledge, the first theoretical study of electron scattering from halo nuclei was presented in ref.[15]. In this reference we developed the formalism focusing on elastic scattering and on exclusive $(e, e'\alpha)$ and (e, e'n) coincidence experiments. In particular we studied the reactions ${}^{6}\text{He}(e, e'\alpha)nn$ and ${}^{6}\text{He}(e, e'n)\alpha n$ using a ${}^{6}\text{He}$ three-body wave function that describes accurately all presently known phenomenology. The results that we present and discuss here are based on that previous work, where details of calculations can be found.

Determination of the spectral function requires coincidence measurements in exclusive experiments. Since the complexity of these experiments is high, it is natural to think that inclusive (e, e') experiments, in which only the scattered electron is detected, will be the ones to be performed first. Moreover, it is difficult to select adequate kinematical conditions for exclusive experiments due to the large number of variables (energy and momentum transfer (ω,q) and energy and direction of the knocked out particle). In this regard it is mandatory to know first what are the (ω,q) domains where the quasielastic peaks for α knockout and halo neutron knockout dominate the total (e,e') differential cross section for the halo nucleus. For the first time we show here results on inclusive scattering over an (ω, q) region that allows to visualize the appearance of different quasielastic e- α and e-n peaks in different kinematical regions. We also show that coincidence measurements in this separate kinematical regions allow to determine the spectral functions of the core and the halo neutrons, and thus the detailed structure of the three-body wave function in momentum space.

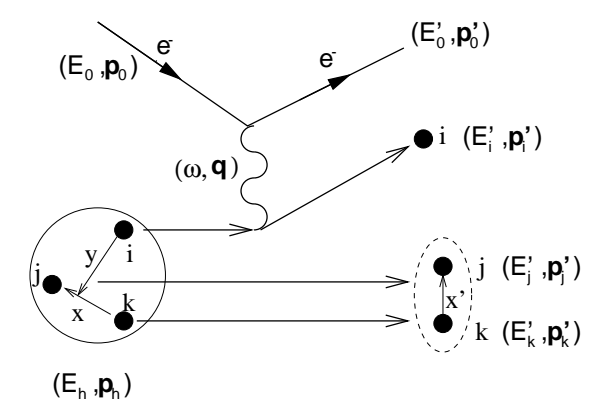


Fig. 1. Scheme and definition of the coordinates used.

2 Model and method

To probe the structure of the three–body wave function of two–neutron halo nuclei we consider the reaction sketched in fig.1. The collision between the electron and the target is taken as a process in which one of the three constituents in the target absorbs the whole energy and momentum transfer (ω, \mathbf{q}) and is knocked out from the target. Core excitations and core breakup reactions are not considered here, and the inclusive cross section

$$\frac{d^3\sigma}{dE_0'd\Omega_{p_0'}} = \sigma_M \left(V_L W_L + V_T W_T \right) \tag{1}$$

can then be computed as the sum of three terms corresponding to the absorption of the virtual photon by each of the three constituents in the halo nucleus. In the same way the structure functions W_L and W_T are given by the sum of the elementary structure functions $W_{L,T}^{(i)}$ corresponding to a process where the constituent i absorbs the virtual photon. In the particular case of ⁶He, since the α -core has zero spin, one has $W_L = 2W_L^{(n)} + W_L^{(\alpha)}$ and $W_T = 2W_T^{(n)}$. In the reaction shown in fig.1 the incident and scattered electrons as well as the ejected particle (constituent i) are described as plane waves (Plane Wave Impulse Approximation). Since we are dealing with a borromean target the residual two-body system made by particles j and k is in the continuum, and the final interaction between them is included in the calculation.

Working in the frame of the halo nucleus ($p_h = 0$) the differential cross section of the process shown in fig.1 is:

$$\frac{d^6 \sigma^{(i)}}{dE'_0 d\Omega_{p'_0} d\Omega_{p'_i} dE'_x} = (2\pi)^3 \frac{p'_i E'_i (m_j + m_k)}{M_h} f_{rec} \sigma^{ei}(\boldsymbol{q}, \boldsymbol{p}_i) S(E'_x, \boldsymbol{p}_i)$$
(2)

where the different momenta and energies are shown in the figure. p'_x is the relative momentum between particles j and k in the final state. m_j , m_k and M_h are the masses of the halo constituents j, k and the total mass of the halo nucleus, respectively. $E'_x = p'^2_x/2\mu_{jk}$ is the kinetic energy of the system made by particles j and k referred to its own center of mass and μ_{jk} its reduced mass. f_{rec} is the recoil factor, $\sigma^{ei}(\mathbf{q}, \mathbf{p}_i)$ is the cross section for elastic electron scattering on constituent i, and $S(E'_x, \mathbf{p}_i)$ is the spectral function.

The cross section $\sigma^{ei}(\boldsymbol{q}, \boldsymbol{p}_i)$ takes the general form $\sigma^{ei}(\boldsymbol{q}, \boldsymbol{p}_i) = \sigma_M(V_L \mathcal{R}_L^{(i)} + V_T \mathcal{R}_T^{(i)} + V_{LT} \mathcal{R}_{LT}^{(i)} + V_{TT} \mathcal{R}_{TT}^{(i)})$, where the V's are kinematic factors and the $\mathcal{R}^{(i)}$'s are structure functions associated to an electron scattering process on constituent i. When this constituent has spin 0 (as the α particle in ⁶He) only the longitudinal structure function appears (see [15] for details).

 $S(E_x', \mathbf{p}_i)$ is the spectral function, that is interpreted as the probability for the electron to remove a particle from the nucleus with internal momentum \mathbf{p}_i leaving the residual system with internal energy E_x' . This function contains the information about the nuclear structure, in particular it contains the whole dependence on the halo nucleus wave function and on the continuum wave function of the residual two-body system. It is defined as the square of the overlap between both wave functions, which reduces to the square of the Fourier transform of the halo wave function when the final interaction between the two surviving constituents is neglected.

The cross section for an inclusive quasielastic electron scattering process is obtained from eq.(2) after integration over the unobserved quantities, i.e. $\Omega_{p'_i}$ and E'_x , and after summation over the index i, that runs over all the three constituents of the halo nucleus, the two neutrons and the core. Since the LT and TT terms in the cross section automatically disappear after integration over $\Omega_{p'_n}$ [16], one immediately recovers the expression in eq.(1).

In what follows we discuss results for $^6{\rm He}$, that is described as a system made by an α -particle and two neutrons. Compared to other halo nuclei $^6{\rm He}$ has the advantage that the interactions between the constituents are well known, and that the α -core is tightly bound. Since the spin of the core is zero we get for $^6{\rm He}$

$$W_L = 2W_L^{(n)} + W_L^{(\alpha)}; W_T = 2W_T^{(n)}$$
 (3)

where

$$W_{\kappa}^{(i)} = (2\pi)^4 \frac{m_j + m_k}{M_h} \int d\theta_{p_i'} dE_x' p_i' E_i' f_{rec} \sin \theta_{p_i'} \mathcal{R}_{\kappa}^{(i)}(\boldsymbol{q}, \boldsymbol{p}_i) S(E_x', \boldsymbol{p}_i)$$
(4)

The neutron structure functions $\mathcal{R}_L^{(n)}$ and $\mathcal{R}_T^{(n)}$ are computed using the CC1 prescription for the nucleon current [17], and their analytic expressions are given in [15]. The structure function $\mathcal{R}_L^{(\alpha)}$ is the square of the Fourier transform of the α -particle charge density. We use the experimental α charge density parameterized as a sum of two gaussians as in table V of [18]. Explicit expressions of the spectral functions $S(E', \mathbf{p}_n)$ and $S(E', \mathbf{p}_\alpha)$ are given by eqs.(33) and (56) of [15]. We use a three-body ⁶He wave function obtained by solving the Faddeev equations in coordinate space. The procedure is shown in detail in [19]. The continuum wave function of the residual two-body system in the final state is written as a partial wave expansion [20] whose radial functions are obtained by solving the Schrödinger equation with the corresponding neutron-neutron or neutron- α potential. For the n-n interaction we use a simple potential with gaussian shape including a central, spin-orbit, spin-spin, and tensor terms, whose parameters are adjusted to reproduce low energy neutron-neutron scattering data. For the n- α interaction we use a potential with central and spin-orbit terms also with gaussian shapes and parameters adjusted to reproduce the phase shifts for s, p, and d waves up to 20 MeV. These potentials provide an accurate description of the available information on ⁶He. Details about these potentials are given in [21].

3 Results

In the upper part of fig.2 we show the longitudinal and transverse structure functions W_L and W_T for varying energy transfer ω at fixed values of the momentum transfer (q=90, 150 and 200 MeV/c). Note that for each q the accessible ω values are constrained to be less than $q(\omega^2-q^2<0)$. In the upper-left part of fig.2 we see that W_L is dominated by the contribution of the α -knockout. The latter is seen as a strong peak centered at $\omega \approx q^2/2m_{\alpha}$, to which we refer as the α -peak. The contribution from the halo neutrons to W_L is not visible at the (ω,q) values considered in this figure. For q>200MeV/c the α -peak decreases while the contribution from the halo neutrons increases with increasing q as the α and neutron form factors, respectively. For q-values beyond 250 MeV/c the α -peak gets shorter and shorter and the contribution to W_L from halo neutrons shows up at $\omega \approx 30$ MeV. However, at this energy and momentum transfer this contribution may have a large overlap with the contribution from core breakup, i.e., from one-nucleon knockout from the α -particle. We have indicated with vertical arrows the ω -values where core breakup contributions may show up more. For ω -values to the left of the arrows W_L is dominated by the α -peak.

The structure function W_T is shown in the upper-right part of fig.2. As already announced, only the halo neutrons contribute to these peaks (we refer to them

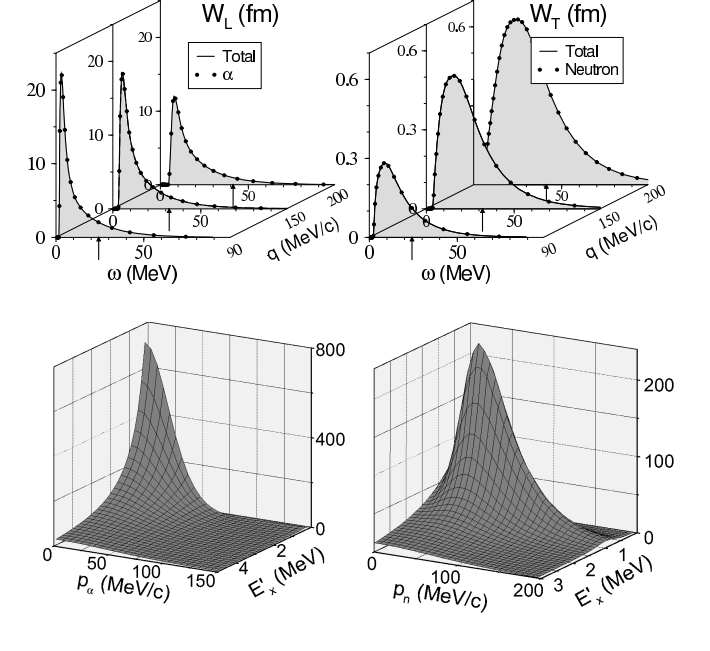


Fig. 2. Upper part: W_L and W_T for momentum transfers q=90, 150 and 200 MeV/c as a function of ω . The dotted lines show the contribution from the α -particle in W_L and from the halo neutrons in W_T . The arrows indicate the ω -values where core breakup contributions may show up. Lower part: Spectral functions for α -knockout (left) and halo neutron knockout (right).

as halo-neutron peaks) which are seen to increase with increasing q-values and are centered at $\omega \approx q^2/2m_n$. Again we indicate by arrows the ω -values where core breakup contributions to W_T will show up more. Core breakup contributions to both W_L and W_T are expected to be more sizeable at q > 250 MeV/c and $\omega > 25$ MeV. Typically data on one nucleon knockout from a free α -particle are available at larger q-values than those considered in fig.2 [22]. An estimate of the core breakup contributions to the W_L and W_T structure functions for inclusive ⁶He(e, e') can be obtained from this reference for 280 MeV/c $\lesssim q \lesssim 720$ MeV/c. The maximum values of W_L and W_T for ⁴He(e, e') extracted from this reference are $W_L \sim 1.5$ fm and $W_T \sim 2$ fm, which take place at $q \sim 360$ -380 MeV/c and $\omega \sim 70$ -80 MeV.

Therefore the low (ω,q) domain shown in the upper plots of fig.2 appears to be optimal to obtain independent and reliable measurements of the α and the halo neutron peaks, and thus on the momentum distributions of the different components of the three–body system. Indeed, as seen in fig.2, W_L provides information about the spectral function $S(E'_x, p_\alpha)$, corresponding to an α –knockout process, while W_T contains information about the spectral function $S(E'_x, p_n)$, corresponding to a halo neutron knockout process. Both spectral functions are shown in the lower part of the figure. From the plots one could naively think that W_T is wider than W_L because of the different widths of the

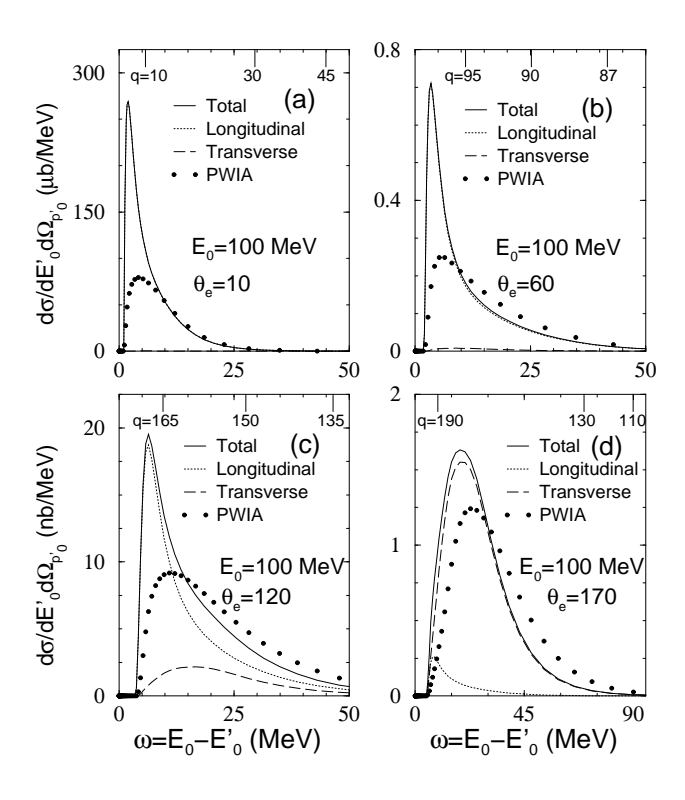


Fig. 3. Differential cross section for E_0 =100 and various scattering angles. The solid lines, short-dashed lines and long-dashed lines are the total cross section, the longitudinal contribution and the transverse contribution, respectively. The dotted line gives is a full PWIA calculation. The q-values in the upper axes are given in MeV/c.

corresponding spectral functions in the lower part of the figure. However the main reason for this is the different mass of core and neutron. The heavier the particle giving rise to a structure function, the narrower the structure function. Since the α -particle is four times heavier than the neutron one has that W_L is narrower than W_T . More details of the spectral functions are discussed in ref.[15]. They could be measured by coincidence experiments ⁶He $(e, e'\alpha)2n$ and ⁶He(e, e'n)⁵He in the low (ω, q) region explored here.

To show that indeed we can get separately information of the α and haloneutron peaks, we show in fig.3 how W_L and W_T enter in the inclusive differential cross section for incoming energies (E_0) and scattering angles (θ_e) adequate to explore the low (ω,q) domain discussed above. In this figure we show the inclusive ${}^6\mathrm{He}(e,e')$ cross section for $E_0=100$ MeV, and four different values of θ_e . There is a clean separation of longitudinal and transverse contributions as one goes from forward angles $(\theta_e=10^\circ, 60^\circ)$ to backward angles $(\theta_e=120^\circ, 170^\circ)$. The results are plotted as a function of ω . For fixed E_0 and θ_e values ω and q are linked by the relation $q^2=\omega^2+4E_0(E_0-\omega)\sin^2(\theta_e/2)$. To guide the reader q-values are indicated in the upper horizontal axes. Similar plots are obtained if one varies the incoming energy in the range 70 MeV $\lesssim E_0 \lesssim$

150 MeV. At forward angles only the α -peak (W_L) contributes, while as θ_e increases beyond 90° the halo neutron contribution (W_T) starts to increase till it becomes the dominant contribution to the differential cross section. At 180° there is no contribution from the longitudinal structure function and the only contribution remaining is the transverse one. This is a general property that is well known and prevails for electron scattering from any target (see for instance ref. [23] and references therein). Not included in these figures is the contribution from elastic electron⁻⁶He scattering, that was considered in [15] and contributes only at forward angles and $\omega \to 0$. We can see in fig.3 that, in each plot, the peak of the differential cross section falls in an (ω,q) range that is expected to be free from core breakup: $q \lesssim 200 \text{ MeV/c}$ and $\omega < q^2/2M_N + S_N$, where M_N is the nucleon mass and $S_N \approx 20$ MeV is the nucleon separation energy in the α -particle. The latter process will be considered subsequently. In the calculations only the final interaction between particles j and k (see fig. 1) is included. The important role that this interaction plays can be appreciated in fig.3 by comparison to PWIA results (dotted line), where this interaction is switched off. The difference between both calculations is due to the structure that the two-body spectator resonances create in the spectral functions. It would be interesting to study the effect caused by the final state interaction between the knocked out particle and the spectators. The treatment of three-body interactions in the final state is highly non-trivial and deserves further work. In particular this requires knowledge of the three-body resonance states. Experimental knowledge of three-body resonances is scant, but progress along these lines is being made [24].

4 Conclusion

In summary, we have investigated inclusive electron scattering on two-neutron halo nuclei, and particularly on ${}^{6}\text{He}$, to explore kinematical regions where the quasielastic processes ${}^{6}\text{He}(e,e'n)\alpha n$ and ${}^{6}\text{He}(e,e'\alpha)nn$ are favored. Considering the halo nucleus as a three–body (core+n+n) system, the differential cross section is calculated as the sum of terms coming from halo–neutron knockout and core knockout. It is then desirable to determine under what conditions the behavior of the different observables, cross section and structure functions, is dominated either by the halo neutrons or by the α -core.

At forward scattering angles, for low q and ω ($q\lesssim 200$ MeV/c, $\omega\sim q^2/m_\alpha$) the behavior of the differential cross section and of the longitudinal structure function is dictated by the α -knockout process. In this domain the cross sections are large and dominated by the α -peak. It is therefore in this region where coincidence $(e,e'\alpha)$ measurements should be performed to determine the spectral function $S(E_x', \mathbf{p}_\alpha)$ that carries the information on the α -momentum distribution in the halo nucleus, or equivalently on the dineutron residual system.

Furthermore, in the $\omega \to 0$ limit elastic scattering from ⁶He will provide the most stringent test of the charge distribution in ⁶He. If the present halo picture is correct the charge distribution in ⁶He must be dictated by that in the α -core.

On the contrary, backward scattering is more favorable to measure the haloneutron peak. In particular, $\theta_e \gtrsim 160^\circ$, $50 \lesssim E_0 \lesssim 100$ MeV and $\omega < 40$ MeV define a region where the inclusive cross section is sizeable and dominated by the halo neutron peak. Thus coincidence (e,e'n) measurements in this region will allow to determine the spectral function $S(E'_x, \mathbf{p}_n)$ that carries the information on the halo neutron momentum distribution, or equivalently on the unbound ⁵He residual system.

The procedure used here will be extended to other halo nuclei in the near future.

This work was supported by DGESIC (Spain) under contract number PB98–0676.

References

- [1] I. Tanihata et al., Phys. Lett. B 160 (1985) 380.
- [2] I. Tanihata et al., Phys. Lett. B 206 (1988) 592.
- [3] P.G. Hansen and B. Jonson, Europhys Lett. 4 (1987) 409.
- [4] L. Johannsen, A.S. Jensen and P.G. Hansen, Phys. Lett. B 244 (1990) 357.
- [5] P.G. Hansen, A.S. Jensen, and B. Jonson, Ann. Rev. Nucl. Part. Sci. 45 (1995) 591.
- [6] M.V. Zhukov, B.V. Danilin, D.V. Fedorov, J.M. Bang, I.J. Thompson, and J.S. Vaagen, Phys. Rep. 231 (1993) 151.
- [7] R. Anne et al., Phys. Lett. B 250 (1990) 19.
- [8] N.A. Orr et al., Phys. Rev. Lett. 69 (1992) 2050.
- [9] N.A. Orr et al., Phys. Rev. C 51 (1995) 3116.
- [10] M. Zinser et al., Phys. Rev. Lett. 75 (1995) 1719.
- [11] T. Nilsson et al., Europhys. Lett. 30 (1995) 19.
- [12] F. Humbert et al., Phys. Lett. B 347 (1995) 198.
- [13] M. Zinser et al., Nucl. Phys. A 619 (1997) 151.

- [14] T. Ohkawa and T. Katayama, Proc. of the Particle Accelerator Conference, Vancouver (1997) 30.
- [15] E. Garrido and E. Moya de Guerra, Nucl. Phys. A 650 (1999) 387.
- [16] J.A. Caballero, T.W. Donnelly and G.I. Poulis, Nucl. Phys. A 555 (1993) 709.
- [17] T. de Forest, Jr., Nucl. Phys. A 392 (1983) 232.
- [18] H. de Vries, C.W. de Jager, and C. de Vries, At. Dat. and Nucl. Dat. Tab. 36 (1987) 495.
- [19] D.V. Fedorov, E. Garrido and A.S. Jensen, Phys. Rev. C 51 (1995) 3052.
- [20] E. Garrido, D.V. Fedorov and A.S. Jensen, Phys. Rev. C 55 (1997) 1327.
- [21] E. Garrido, D.V. Fedorov and A.S. Jensen, Nucl. Phys. A 617 (1997) 153.
- [22] S.A. Dytman et al., Phys. Rev. C 38 (1988) 800.
- [23] E. Moya de Guerra, Phys. Rep. 138 (1986) 293.
- [24] T. Aumann et al., Phys. Rev. C 59 (1999) 1252.